physical variable or a constructed variable precedes this step is immaterial.

Acknowledgment

This work was supported under Air Force Contract F49620-79-C-0054.

References

[1] Van Dyke, M. D., *Perturbation Methods in Fluid Mechanics*, Annotated Edition, Parabolic Press, Stanford, Calif., 1975.

[2] Lighthill, M. J., "A Technique for Rendering Approximate Solutions to Physical Problems Uniformly Valid," *Zeitschrift für Flugwissenschaften*, Vol. 9, Sept. 1961, pp. 267-275.

AIAA 81-4065

Improved Measurement of Turbulent Intensities by Use of Photon Correlation

G. D. Catalano*
Air Force Wright Aeronautical Laboratories, Wright-Patterson AFB, Ohio
and
R. E. Walterick† and H. E. Wright‡
Air Force Institute of Technology, Wright-Patterson AFB, Ohio

Introduction

MEASUREMENTS of turbulent intensities exceeding 30% are now realizable using a laser velocimeter and frequency shifting device such as a Bragg cell. In addition, by using the photon correlation processing scheme, the turbulent measurements can be made in complex flowfields with recirculation regions.[1] The photon correcting techniques offer improved sensitivity compared to frequency counter and tracker processes by permitting velocity measurements to be made even when insufficient signal photons are available to define the classical scattering signal. Naturally occurring contaminant particles are used as scatterers with no artificial seeding introduced.

One of the primary disadvantages of the photon correlation scheme is that all of the turbulent information must be obtained from the autocorrelation function of the fluctuating velocity field. In fact, the location and relative amplitude of the first several maxima and minima are necessary to determine the local mean velocity and the local turbulent intensity. If the autocorrelation function is skewed or distorted for any of several often occurring reasons, the credibility of the data obtained is then open to challenge.

The purpose of this Note is to describe one approach to improving the accuracy of the turbulent information obtained from the autocorrelation function. Polynomial curve fitting and then averaging is used to eliminate the function distortion.

Equipment and Experimental Procedure

This experiment is performed in the near field region of a two-dimensional turbulent wake flow. A cylinder 11.75 cm in diameter is placed in the test section whose dimensions are 7.0 cm wide by 150.0 cm long. The tunnel flow is kept at a constant velocity of 5.9 m/s with the Reynolds number equal to 48,000 based on the cylinder diameter. Measurements are made at several downstream locations.

The optical arrangement is shown in Fig. 1. A lens with a focal length of 100 cm is used with the beam separation equal to 2 cm. The laser used is a 15 mW helium neon type. Careful alignment of the photomultiplier tube is performed in order to achieve a maximum signal level.

The signal from the photomultiplier tube is passed directly to a Malvern correlator. The correlator is used to determine the autocorrelation functions of the turbulent velocity field.

The power spectra as found by Lumley et al.[2] is

$$P(w) = \tfrac{1}{4}[\exp\{-(w+w_0)^2a^2/2\} + \exp\{-(w-w_0)^2a^2/2\} \quad (1)$$

where w_0 is the Doppler frequency, and a is a constant.[3] Taking the Fourier transform yields the autocorrelation function

$$R(t) = \exp(-t^2/2a^2)\cos(w_0 t) \quad (2)$$

Consider the case when the autocorrelation curve has been distorted by either a lack of number of fringes in the control volume or significant background scattered light (Fig. 2). The calculation of the turbulent intensity from an autocorrelation function can be approximated by determining the decrease in the amplitude of the cosine-like wave. One approximation[4] used is the following

$$\frac{u_{\rm rms}}{U} = \frac{1}{\pi}\left(\tfrac{1}{2}(R-1) + \frac{1}{2n^2}\right)^{\frac{1}{2}} \quad (3)$$

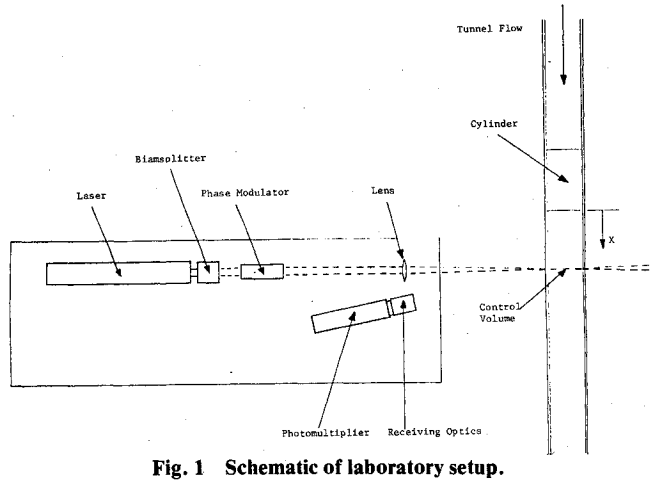

Fig. 1 Schematic of laboratory setup.

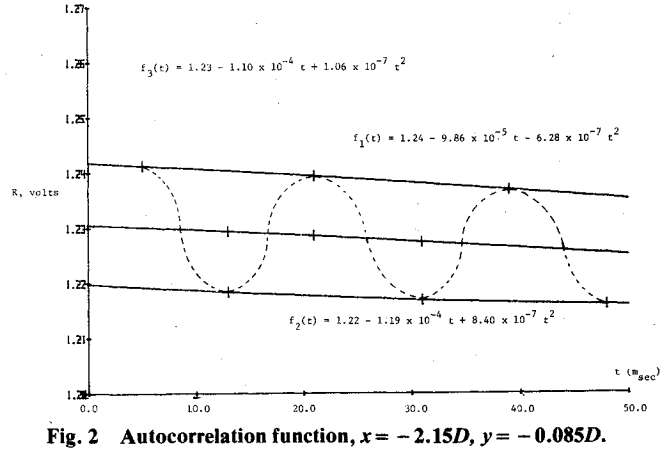

Fig. 2 Autocorrelation function, $x = -2.15D$, $y = -0.085D$.

Received Aug. 7, 1980. This paper is declared a work of the U. S. Government and therefore is in the public domain.

*Aerospace Engineer, Aeromechanics Division.
†Graduate Student, School of Engineering.
‡Professor, School of Engineering.

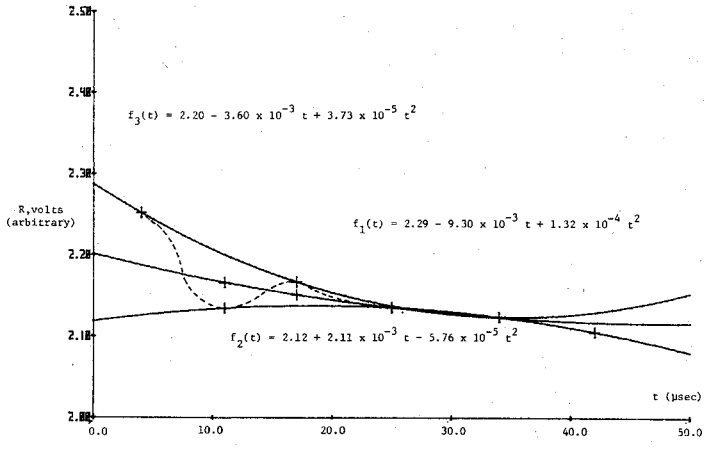

Fig. 3 Autocorrelation function, $x=0.5D$, $y=0D$.

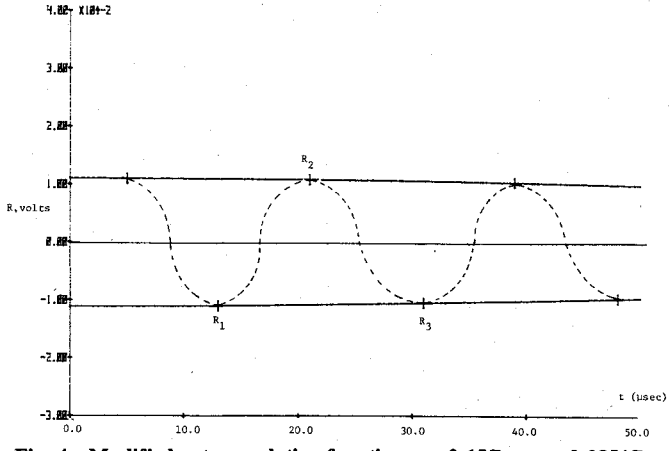

Fig. 4 Modified autocorrelation function, $x=2.15D$, $y=-0.0851D$.

where

$$R=\frac{R_2-R_1}{R_2-R_3}$$

and R_1, R_2, and R_3 correspond to the voltage(s) at the first minimum, the first maximum, and the second minimum locations, and n is the number of fringes in the control volume. Note that if the autocorrelation curve is skewed or distorted, the absolute value of the voltage R_3 may be less than the absolute value of the voltage, R_1. For $|R_3| < |R_1|$, the value of R is less than unity with Eq. (3) resultantly undefined.

Intuitively, this would seemingly indicate a growth in the amplitude of the cosine wave that is not physically realizable for a turbulent autocorrelation function. Thus the need exists to eliminate this skewness.

The approach used is to fit a second-order polynomial curve through the first several maxima and another second-order polynomial curve through the first several minima. That is,

$$f_1(t_{\max}) = a_1 + a_2 t_{\max} + a_3 t_{\max}^2 \tag{4}$$

and

$$f_2(t_{\min}) = b_1 + b_2 t_{\min} + b_3 t_{\min}^2 \tag{5}$$

The constants are then determined from the measured maxima and minima voltages.

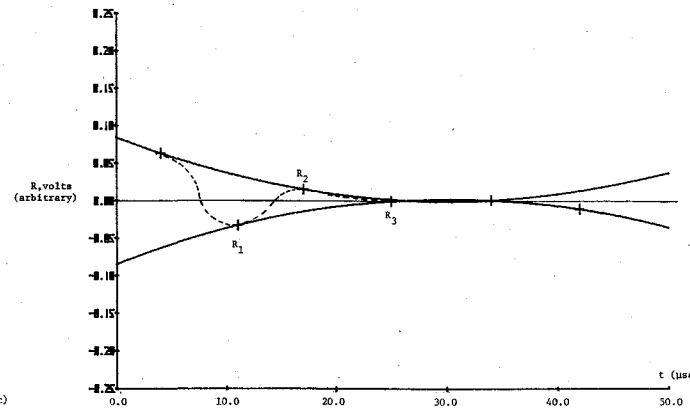

Fig. 5 Modified autocorrelation function, $x=0.5D$, $y=0D$.

The polynomials are next averaged yielding

$$f_3(t_{\text{avg}}) = c_1 + c_2 t_{\text{avg}} + c_3 t_{\text{avg}}^2 \tag{6}$$

where

$$c_1=\frac{a_1+b_1}{2}, \qquad c_2=\frac{a_2+b_2}{2}, \qquad c_3=\frac{a_3+b_3}{2} \tag{7}$$

The function $f_3(t_{\text{avg}})$ can be considered the new reference datum for the autocorrelation function. By subtracting the voltages corresponding to the appropriate t values, the autocorrelation curve is then centered about the zero reference level. That is

$$R_{\text{new}}(t) = R_{\text{old}}(t) - f_3(t) \tag{8}$$

Now the voltage maxima and minima can be calculated and used in Eq. (3) to determine the turbulent intensity.

Experimental Results

The data analysis scheme is tried in the determination of turbulent intensities in the near field region of a two-dimensional wake. Two examples of the resultant autocorrelation functions are shown in Figs. 2 and 3. The autocorrelation function in Fig. 2 is measured at the flowfield location $X/D=-2.15$ and $Y/D=-0.085$ while the function in Fig. 3 is obtained at the location $X/D=0.5$ and $Y/D=0$.

For the first flowfield location, the mean velocity $\overline{U}$ is calculated to be 5.86 m/s. However, the turbulent intensity is undefined using Eq. (3). In Fig. 3, for the second downstream location, the mean velocity $\overline{U}$ is -1.0 m/s and the turbulent intensity $u_{\text{rms}}/\overline{U}$ is calculated to be equal to 0.21.

Second-order polynomials are then fitted to the maxima and minima points with the resultant modified autocorrelation functions being displayed in Figs. 4 and 5, respectively. The mean velocities remain unchanged but the turbulent intensities do take on new values. At the first flowfield location $X/D=-2.15$ and $Y/D=-0.085$, $u_{\text{rms}}/\overline{U}$ is equal to 0.01 while at the location $X/D=0.5$ and $Y/D=0$, $u_{\text{rms}}/\overline{U}$ is equal to 0.4.

Conclusions

The data analysis scheme proved efffective in the determination of turbulent intensities in the cases when the autocorrelation function is skewed due to few fringes in the control volume or significant background light entering the collecting optics.

References

[1]Morris, S. L., "Flow Field Diagnostics Behind a Bluff Body Utilizing Photon Correlation," M. S. Thesis, Air Force Institute of Technology, Wright-Patterson AFB, Ohio, Dec. 1979.

[2]Lumley, J., George, W., and Kobashi, Y., "A Theoretical Description of Autocorrelation Function," *Proceedings, Symposium of Turbulence in Liquids,* University of Missouri at Rolla, Plenum Press New York, 1970.

[3]Morton, J. B., "Experimental Measure of Ambiguity Noise in a Laser Anemometer," *Journal of Physics E: Scientific Instruments,* Vol. 6, No. 4, pp. 346-348.

[4]Abbis, J., Piks, E. R., "Laser Anemometry," *Malvern Digital Correlator Operating and Installation Manual,* Malvern Instruments Limited, Worcestershire, England, pp. 6.1-6.6.

AIAA 81-4066

Double-Diaphragm Shock Tube: Comparison between Theory and Experiment

Anthony W. Hodgson* and John C. Mackie†
University of Sydney, Sydney, Australia

THE double-diaphragm shock-tube technique developed by Holbeche[1,2] is an ideal way to cool shock-heated gases and vapors rapidly. It has been used to study vibrational relaxation[1-4] and atomic recombination reactions,[5,6] and is also suitable for the study of homogeneous nucleation.

The usefulness of the technique, however, depends on knowing the flow properties throughout the region of interest. Treatments so far have assumed that shock reflection from the second diaphragm can be ignored. We describe a series of experiments performed to establish the presence of a reflected shock from the second diaphragm and give brief details of the theoretical analysis used to obtain flow properties.

The shock tube of 76 mm diameter (see Fig. 1) has been described elsewhere.[6] A scored aluminum disk and two sheets of 0.025 mm aluminum foil were used for primary and secondary diaphragms, respectively. Pressure was measured by Kistler piezoelectric pressure transducers mounted 80 mm upstream and 100 and 455 mm downstream from the secondary diaphragm. Light scattered at 90 deg from an argon ion laser beam (476.5 nm) was also recorded 455 mm downstream from the secondary diaphragm. In each run high-purity argon and nitrogen were used as test and driver gas, respectively.

Pressure measurements upstream from the secondary diaphragm indicate that shock reflection has occurred. A typical oscilloscope trace showing pressures upstream and downstream of the secondary diaphragm is given in Fig. 2. Previous analyses assumed no shock reflection. Inclusion of shock reflection in the flow analysis necessitates a full method of characteristics analysis, similar to that of Rudinger.[7]

In our analysis, the incident shock reflects from the secondary diaphragm (assumed planar) and travels back upstream into the test gas. At a later stage, the secondary diaphragm bursts instantaneously due to the increased pressure behind the reflected shock. A rarefaction wave is thus generated, the head of which travels upstream into the test gas; the tail travels downstream into the evacuated expansion section. The rarefaction wave head eventually catches up to the reflected shock front, and the resulting interaction causes the shock wave to decay.

Particle paths are constructed through the characteristics mesh so that gas properties at any point in time and space are known. In particular, gas temperature and pressure at the point where each path passes an observation position are calculated and theoretical pressure profiles thus obtained. The various features of the flow are shown in Fig. 1.

Comparison of experimental pressure traces with theoretical profiles where shock reflection has and has not been considered is made in Fig. 2. It may be seen that downstream of the secondary diaphragm both theoretical treatments fit the trace well apart from a timeshift (discussed later). However, upstream there is a marked difference—the arrival of the reflected shock front can clearly be seen in the experimental pressure trace.

In the analysis described above, the time between shock reflection and secondary diaphragm bursting (the bursting time) is not directly determinable. However, the time between the arrival of the incident and reflected shocks at the upstream window (Δt) is a function of bursting time. Bursting time can therefore be obtained by fitting a theoretical Δt value to the experimental value. It was found that bursting times were typically between 15 and 35 μs.

In each run it was possible to fit the downstream theoretical pressure profiles to the experimental trace by shifting it by times of between 60 and 180 μs. Profiles where shock reflection was and was not taken into account fitted the experimental data equally well. This time shift has been observed by a number of earlier workers.[1,2,6,8] Beck,[6] using the same apparatus, found time shifts of between 85 and 175 μs were necessary, while Nasser[8] needed about 45 μs to fit his data. In their study of water condensation in a driver expansion, Glass et al.[9] also found it necessary to shift their

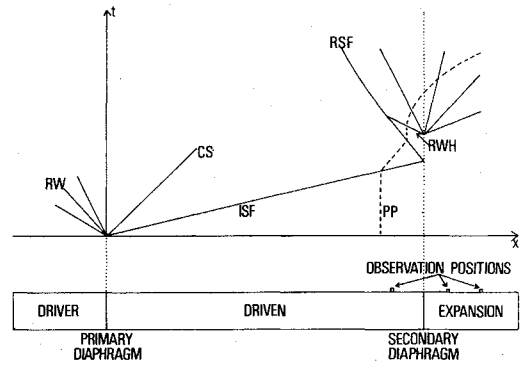

Fig. 1 Gas flow in double-diaphragm shock tube (incident (ISF) and reflected (RSF) shock fronts, contact surface (CS), rarefaction wave generated by rupture of primary diaphragm (RW), head of rarefaction wave generated by rupture of secondary diaphragm (RWH), and particle path (PP) are shown).

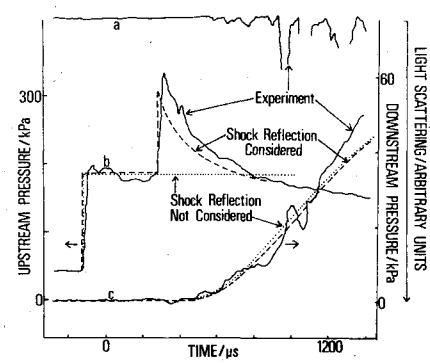

Fig. 2 Typical oscilloscope traces: a) light scattering, and pressure at b) upstream and c) downstream observation positions. Experimental pressure traces (—) are compared to theoretical profiles where shock reflection has (– – –) and has not (·····) been considered. (Time shift of 120 μs was made in theoretical downstream pressure profiles; zero in time corresponds to rupture of secondary diaphragm.)

Received May 13, 1980; revision received Sept. 9, 1980.

*Graduate Student, Dept. of Physical Chemistry.
†Associate Professor, Dept. of Physical Chemistry.